

Article

Outage Survivability Investigation of a PV/Battery/CHP System in a Hospital Building in Texas

Kazi Sifatul Islam ^{1,2}, Samiul Hasan ^{2,3,4}, Tamal Chowdhury ¹, Hemal Chowdhury ^{2,3,*} and Sadiq M. Sait ⁵ 

¹ Department of Electrical and Electronic Engineering, Chittagong University of Engineering & Technology (CUET), Chattogram 4349, Bangladesh

² Bangladesh Steel Re-Rolling Mills Ltd. (BSRM), Mirsharai, Chattogram 4324, Bangladesh

³ Department of Mechanical Engineering, Chittagong University of Engineering & Technology (CUET), Chattogram 4349, Bangladesh

⁴ Institute of Energy, University of Dhaka, Dhaka 1000, Bangladesh

⁵ Center for Communication and IT Research, Research Institute, King Fahd University of Petroleum & Minerals, Dhahran 31261, Saudi Arabia

* Correspondence: u1303031@student.cuet.ac.bd

Abstract: Climate change and the associated global warming raise the possibility of weather-related natural disasters. Power outages due to natural catastrophes cause substantial financial loss. Moreover, an uninterrupted power supply is essential in disaster-prone areas to continue rescue and other humanitarian activities. Therefore, energy systems must be resilient to withstand power outages due to natural events. Resilience and enhancement techniques, and schemes of integrated electricity and microgrids' heat demand during power outages, were mainly overlooked in the earlier analysis. Therefore, this analysis aims to analyze a grid-tied microgrid's survivability during a power outage due to a natural disaster in Texas, USA. Mixed-integer linear programming (MILP) is used to optimize various energy resources, such as PV, battery, grid, and combined heat and power (CHP) for Texas, USA. These technologies were run in an outage condition to observe their resiliency benefits. To determine the resilience performance of the CHP/PV/battery system for the hospital building, a new probabilistic approach was applied. A 24-h outage was simulated in REopt lite software, and this study found that the PV/battery/CHP system could easily withstand the outage. The optimum system consists of 3933 kW of PV, 4441 kWh of storage, and a CHP unit having a capacity of 208 kW. The proposed microgrid emits 79.81% less CO₂ than the only grid system. The microgrid has a net benefit of \$1,007,204 over the project duration. The introduction of the proposed microgrid will bring about life-cycle savings (LCS) of 37.02 million USD over the project's lifespan.

Keywords: power outage; REopt; CHP; survivability; critical load; natural disasters



Citation: Islam, K.S.; Hasan, S.; Chowdhury, T.; Chowdhury, H.; Sait, S.M. Outage Survivability Investigation of a PV/Battery/CHP System in a Hospital Building in Texas. *Sustainability* **2022**, *14*, 14965. <https://doi.org/10.3390/su142214965>

Academic Editors: Tomasz Cholewa, Alicja Siuta-Olcha, Dorota Anna Krawczyk, Łukasz Amanowicz and Michał Turski

Received: 11 October 2022

Accepted: 10 November 2022

Published: 12 November 2022

Publisher's Note: MDPI stays neutral with regard to jurisdictional claims in published maps and institutional affiliations.



Copyright: © 2022 by the authors. Licensee MDPI, Basel, Switzerland. This article is an open access article distributed under the terms and conditions of the Creative Commons Attribution (CC BY) license (<https://creativecommons.org/licenses/by/4.0/>).

1. Introduction

Since 1960, the world has seen a ten-fold rise in natural disasters. An Institute for Economics and Peace study revealed a rise in incidents from 39 in 1960 to 396 in 2019 [1]. Among different countries, the United States has seen tremendous growth in natural disasters occurring, and among different regions, Texas is the worst victim of natural disasters. One hundred thirty-seven natural disasters have occurred in Texas until now, and due to this, Texas has incurred a \$200–\$340 billion financial loss [2]. Electrical power networks are usually liable for these severe natural disasters, particularly weather-related incidents. Recent grid outages in Texas due to ice storms show that dependence on the utility grid should be minimized [3]. Instead, the focus should be put more on decentralized energy resources [4,5]. Hence, a microgrid is influential in keeping the power supply on and stable in these situations [6,7].

There is a strong desire to design optimum energy generation and configurations for modern interconnected systems, considering multiple energy sources to provide a resilient,

cheap, and dedicated power supply. Due to the blessings of multi-energy microgrids (mMG), the coordinated use of renewable energy generators, energy storage, and conventional energy has seen tremendous progress in all stages of life [8]. Due to the intrinsic character of how energy technologies are embedded, mMG stands for a noteworthy conversion from traditional methods to hybrid modelling and the techno-economic assessment of energy systems. Along with this, the resilience of microgrids has gained attention among researchers nowadays. Several researchers in the literature have highlighted the resiliency benefits of the microgrid. Ogunmodede et al. have proposed an optimized system for a hospital in San Diego. The optimum system consists of 3152.40 kW of PV and 728.97 kW of battery, and the system can save up to \$2,702,748 [9]. McLaren et al. identified the economic benefit of a solar integrated storage system. This study stated that demand charge reductions result in substantial financial savings from storage-only projects [10]. The reliability of PV/battery systems integrated with diesel generators has been analyzed by Marqusee et al. [11]. This study found that hybrid microgrids provide more resilience than diesel-only systems. A new optimization scheme and resilience index were proposed by Hussain et al., which successfully fulfills the critical load demand during the outage period, taking into account uncertainties and incremental costs within three different network topologies [12]. Amin Khodaei also assessed the minimization of load curtailment, cost deduction, and local load supply as a resilience measure to assure optimal microgrid scheduling during the primary grid's inactivity [13]. Lagrange et al. analyzed that \$440,191 could be saved by a microgrid consisting of PV, lithium-ion batteries, and diesel generators over the project's life span. [14]. Similarly, after identifying the significance of resilience for a commercial building, Laws et al. proposed that an LCS of \$50,000 could be made after implementing PV and batteries [15]. Likewise, Rosales-Asensio et al.'s study observed that a microgrid consisting of PV/battery at an office building can survive a 4-h outage, and over the project's lifetime can save \$ 112,410 [16]. Anderson et al. determined the resilience benefit of a micro-grid for a wastewater treatment plant in North Carolina and found that the microgrid consisting of a hybrid combined-heat-and-power, PV, and storage system can reduce life-cycle energy costs by 3.1% [17]. Similarly, Anderson et al. also included energy justice value in the techno-economic analysis of microgrids. They found that when job creation, health, climate, and resilience costs are included, renewable microgrids help reduce diesel fuel costs and emissions [18]. Hervas-Zaragoza et al. proposed a microgrid consisting of PV and diesel generators to improve the energy resilience of hospital buildings in the post-COVID era [19]. This study found that the proposed system integrated with batteries can endure an average outage of 72 h. Another study analyzed different building patterns and renewable energy sources to report that the possibility of withstanding an outage greatly depends on site-dependent sustainable energy sources and load patterns [20].

The available literature has successfully pointed out the microgrid's resilience advantages. However, the resilience and enhancement techniques, and schemes of integrated electricity and microgrids' heat demand during power outages, were mainly overlooked in earlier works. Only one study is available which addresses this issue [21]. This study aimed to fill this gap by performing a resilience analysis of a hypothetical hospital building consisting of CHP/PV/battery for a hospital building in Texas. For this purpose, a new probabilistic approach was applied to determine the resilience performance of the CHP/PV/battery system for the hospital building, which was missing in [21]. In this analysis, we considered a hypothetical hospital. The hospital is deemed grid-connected to the base case, and only grid-supplied electricity can fulfil all the loads (electrical and thermal). The hospital has five floors and an area of 241,351 ft². Annual electricity consumed by the hospital is 9,011,047 kWh, while the annual heating system fuel consumption is 9641 MMBtu. In Texas, the hottest month is observed in August, and the coldest month is observed in January. Following this, the system's annual electric and heating load profiles are generated and can be found in Figures 1 and 2. The load profile of the building is taken from DOE Commercial Reference Building (CRB) [22]. The highest electrical load is

1704.15 kW, and it was recorded in August. On the other hand, the average heating load is 1.10 MMBtu/hr, and the maximum heating load is 3.99 MMBtu, observed in January. The selected hospital's critical load is estimated to be 50%. The load that must be met in the event of a grid outage is the critical load. A hospital has a variety of loads, such as heaters for the rooms, air conditioners, fans, lighting, and water heaters. In addition, refrigerators must be operational at all times since they store vaccines and medicines. A back-up power system based on renewable energy can play vital roles during a power outage to ensure continuous operations in hospital buildings.

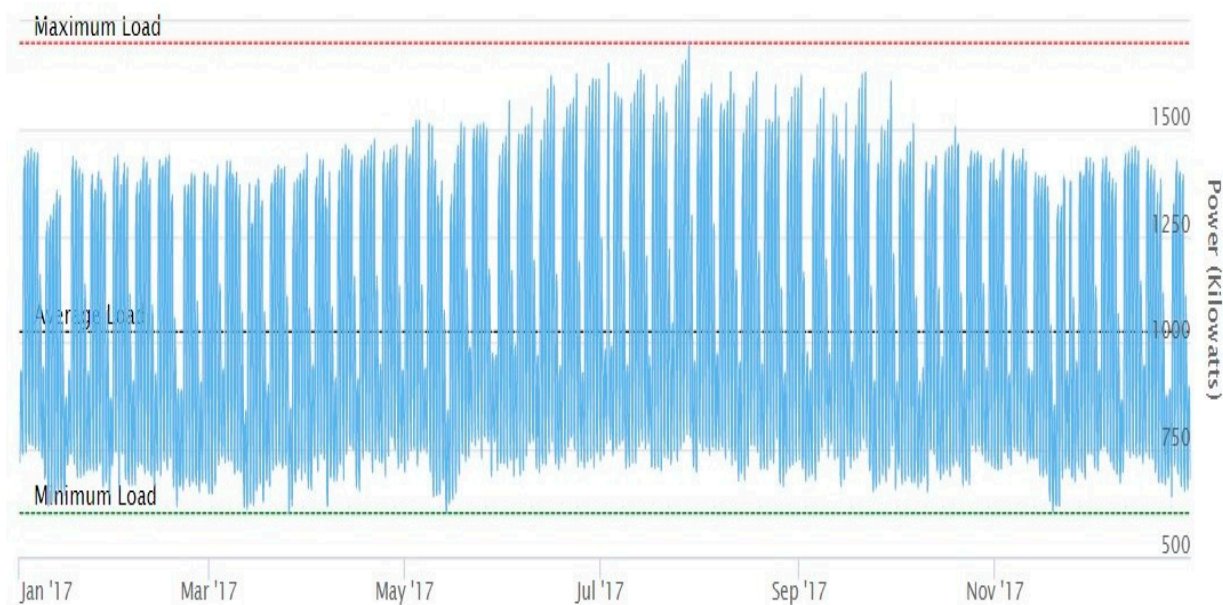


Figure 1. Annual electricity consumption of the hospital building.

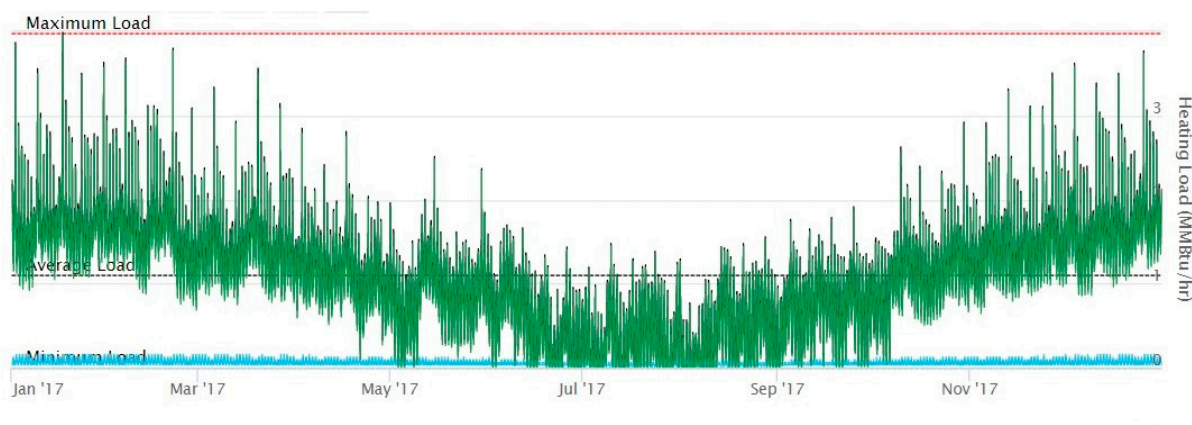


Figure 2. Annual heating energy consumption of the hospital building.

2. Method

2.1. REopt Lite

This study uses REopt Lite, which is MILP optimization, to evaluate the distributed energy resource system's dispatch strategy and its optimum size [22]. This process has two modules: the optimization module (OM) and the simulation module (SM). In the OM module, a site's life cycle energy costs (LCC) are minimized while ensuring the system fulfills the critical loads during a predefined outage period without the help of the utility grid. Two types of analysis, such as resilience and financial, are carried out in the OM module. Financial analysis optimizes the dispatch strategy and its optimum size to minimize the LCC of a site. The same process is also conducted in the resilience analysis,

but with the additional constraint that the system must fulfill the critical loads during a predefined outage period without the help of the utility grid.

OM-recommended technologies and their sizes are taken as inputs in the SM module. The module then determines the annual resilience performance of the system by simulating outages beginning every hour of the year (8760 times). The significant difference between the OM and the SM is the modelling technology. The outage period, system size, and dispatch strategy are fixed in the OM. In comparison, the SM takes in system size and simulates outages beginning every hour of the year rather than a single outage.

In every outage simulation, load following strategy is implemented to evaluate the hourly dispatch. The optimization problem tackled in this study is provided below [22].

$$\min LCC = \min(C_{Eg} + C_{OM} + C_{Dn} + C_{PVBAT}) \quad (1)$$

$$C_{Eg} = \sum_{l \in \mathcal{L}, h \in \mathcal{H}} (F_{ilh}^{pd} * P_{ilh} * c_h^e) \quad (2)$$

$$C_{PVBAT} = \sum_{t \in \mathcal{T}} (X_t * c_t) + (B^{kWh} * c_{kWh}^b) + (B^{kW} * c_{kW}^b) \quad (3)$$

$$C_{Dn} = \sum_{r \in \mathcal{R}} (d_r * c_r^d) + \sum_{m \in \mathcal{M}} (d_m * c_m^d) \quad (4)$$

$$C_{OM} = \sum_{t \in \mathcal{T}} (X_t * c_r^{OM}) \quad (5)$$

To minimize the LCC, the following load constraint equations are used:

$$\sum_{t \in \mathcal{T}} (F_{tlExh}^{pd} * P_{tlExh} * F_t^{dgr}) \leq L_{lh}, \forall h \in \mathcal{H} \quad (6)$$

$$\sum_{t \in \mathcal{T}} F_{tlR_h}^{pd} * P_{tlExh} * F_t^{dgr} + B_h^- \leq L_{lh}, \forall h \in \mathcal{H} \quad (7)$$

$$\sum_{h \in \mathcal{H}} F_{CPVlh}^{pd} * P_{CPVlh} * F_{CPV}^{dgr} \leq \sum_{h \in \mathcal{G}} L_{lSh}, \forall l \in \mathcal{L} \quad (8)$$

Equation (6) allows the total on-site energy to be less than or equal to the highest load of all energy sources for each stage. Equation (7) dictates the grid, PV, CHP, and batteries to fulfil the location's load every time, while Equation (8) requires the power produced by the CHP and PV to be less than or equal to the hospital's load. Finally, the generation constraint is represented by Equation (9), ensuring that CHP's and PV's delivered power equals the system size selected in each stage across all loads.

$$\sum_{l \in \mathcal{L}} P_{tlh} \leq X_{th}, \forall h \in \mathcal{H} \quad (9)$$

The charging, discharging, degradation, and status of battery charge during each sample interval constraints of storage technology are represented by the following equations. When the storage is being charged, the value of Z_h^{B+} will be 1. The discharging of the storage technology will be indicated, if the value of Z_h^{B-} becomes 1.

$$B_h^+ = \sum_{t \in \mathcal{T}} (F_{tlB_h}^{pd} * X_t * F_t^{dgr} * \eta_B), \forall h \in \mathcal{H} \quad (10)$$

$$B_h^{SOC} = B_{h-1}^{SOC} + B_h^+ - B_h^-, \forall h \in \mathcal{H} \quad (11)$$

$$B_h^- \leq B_{h-1}^{SOC}, \forall h \in \mathcal{H} \quad (12)$$

$$Z_h^{B+} + Z_h^{B-} \leq 1, \forall h \in \mathcal{H} \quad (13)$$

Demand rate restrictions are shown by the next two equations. The demand should be greater than or equal to the amount of grid electricity used each month.

$$\sum_{h \in \mathcal{H}_r, l \in \mathcal{L}} P_{Gth} \leq d_r, \forall r \in \mathcal{R} \quad (14)$$

$$\sum_{h \in \mathcal{H}_m, l \in \mathcal{L}} P_{Gth} \leq d_m, \forall m \in \mathcal{M} \quad (15)$$

Fuel consumed by all fuel bins and technology during the operational hour should equal the generated energy multiplied by the fuel burn rate (R) plus the fixed fuel use. This association over all time steps, locations and loads is specified by the following equations:

$$\sum_{h \in \mathcal{H}, s \in \mathcal{S}} F_{lth}^p P_{lsth} F_{ltsu}^R + \sum_{h \in \mathcal{H}, l \in \mathcal{L}} X_{lth}^o F_{ltsu}^f = P_{ltsu}^U, \forall l \in \mathcal{L}, t \in T, u \in U \quad (16)$$

Equation (17) P_{ltsu}^U represents the magnitude of fuel used, and it should be less than the quantity of fuel allocated Q_{ltsu}^U for each technology and fuel bin.

$$P_{ltsu}^U \leq Q_{ltsu}^U, \forall s \in \mathcal{S}, t \in T, u \in U \quad (17)$$

Some of the pertinent constraints listed in [22] are taken into consideration in this study. Only PV, battery, and CHP technology constraints are considered in this study. Another technology, such as wind, is not considered in this study. The main inputs and outputs of the used software can be found in Figure 3.

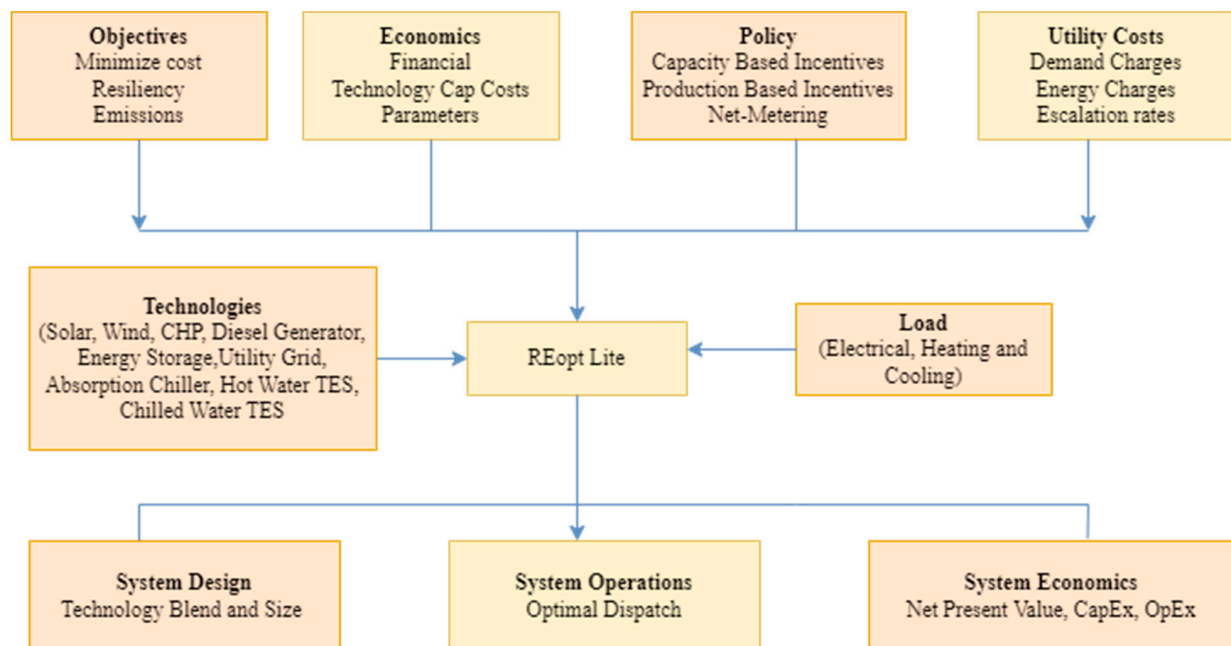


Figure 3. Inputs and outputs of the REopt software.

2.2. Modelling of the System

2.2.1. CHP

In this study, topping cycle CHP is designed, and this is a system that uses fuel to generate electricity and capture waste heat from combustion to support the site thermal load. A cycle diagram of a topping cycle CHP is provided in Figure 4. A CHP plant's electricity and heat generation can be found in the following interaction 18 [8].

$$Q_{out} = \left(\frac{\eta_h}{\eta_e} \right) P_{out} h_c^f \quad (18)$$

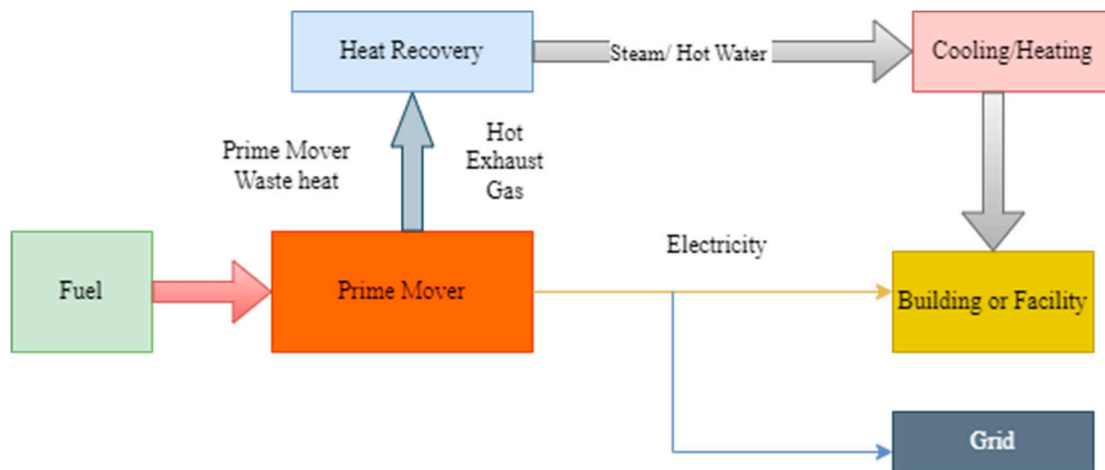


Figure 4. Cycle diagram of a topping cycle CHP.

Both heat and electrical efficiency are nonlinear in general. The electrical efficiency is the ratio of power output to fuel burn rate, while heat recovery efficiency is the ratio of heat output to fuel consumption rate. At light loads, the electrical efficiency is poor; at no load is zero, while at full load, the efficiency rises to a peak. Hence, a linear equation fitting to the fuel burn rate (MMBtu/hr) vs. load data correctly models this changing efficiency. The maximum amount that can be recovered from the system is designed here like the fuel burn rate is. A CHP plant heat recovery rate and fuel burn rate can be designed using the following Equation (19) [8].

$$R_{e,h} = a_{e,h}P_{out} + b_{e,h} \quad (19)$$

At time t , $a_{e,h}$ and $b_{e,h}$ are calculated utilizing heat recovery efficiency and electrical efficiency at the half and full loading conditions. The CHP unit can run simultaneously with the utility to meet any, all, or none of the electrical load. However, in case of a grid outage, it should fulfil all the system's critical load. The existing boiler is a hot water type fueled by natural gas, and the CHP unit is also run by natural gas. The prime mover of the CHP unit is a reciprocating engine with size class 2 (100–630 kW).

2.2.2. Battery

A battery is required to store energy due to the intermittent behavior of renewable sources. During the unavailability of the solar resource, the battery can serve as an essential tool to supply the required power. The necessary battery size for storing power can be found in the following equation.

$$C_{ap_{bat}} = \frac{E_{load}DA}{\eta_{con}n_{batt}DOD} \quad (20)$$

A lithium-ion battery is considered in this analysis. It is anticipated that the storage will last for ten years. The capital cost of the battery is considered to be \$419 per kW [23], and the battery's power capacity cost is considered to be \$775 per kW [22]. The battery's initial state of charge (SoC) should be 50%, and the SoC minimum should be 20%. It is also assumed that during the system lifetime the inverter is replaced once, and the replacement cost is amortized into annual O&M costs. The inverter efficiency is considered 96% [22].

2.2.3. Grid

To supply an unlimited amount of power, a grid is an ideal source. The grid is available in the selected location, which is why the grid's capital and maintenance cost is not considered in this model. Coleman County Elec Coop, Inc-Small Commercial is

considered the power supply provider. The following equation represents the electricity supplied by the grid [24].

$$P_g(t) = P_l(t) - \sum(P_{PV}, P_{batt}, P_{chp}) \quad (21)$$

2.2.4. PV Module

The energy available in the solar resource can be converted into electricity by a PV module. Power available from a solar module can be found from the following interaction [8].

$$P_{PV} = C_{PV} D_{PV} \left(\frac{I_r}{I_{rSTC}} \right) [1 + \alpha_P (T_C - T_{C,STC})] \quad (22)$$

To determine the PV efficiency under standard test conditions and maximum power, Equation (23) can be utilized [8].

$$\eta_{STC} = \frac{C_{PV}}{A_{PV} I_{rSTC}} \quad (23)$$

The solar panel's capital costs are considered as \$310 per kW, and it is anticipated that PV modules will exist for 25 years. Operational and maintenance (O&M, \$/kW per year) costs are considered to be \$17 [22]. Tracking arrangements are not considered for this investigation. Additionally, it is anticipated that the solar panels will not be installed on the hospital's roof but on the ground. The excess energy produced by the PV unit would be reduced after charging the battery and meeting the load demand because net energy metering is not taken into account in this analysis. In REopt, the PVWatts program from NREL is utilized to calculate the installed PV systems' electricity output. One MW-DC of PV is anticipated to be deployed for every 2.42811 hectares of accessible space. DC to AC size ratio is considered 1.2 and the system loss is 14% [22].

2.2.5. Probabilistic Approach

The number of hours that a system has survived an outage is represented by each value in an array of length 8760 for hourly analysis, denoted by r , where individual value in the array represents the total survival hours of the system for the outage beginning in the $[index + 1]$ i th hour. The probabilities of survival for outages of different durations are computed using the following formula (Equation (24)) after computing the survived outage duration's (or r) series [25].

$$P(hrs_i) = \frac{1}{ts} \sum_{h \in r} \begin{cases} 1, & \text{if } h > hrs_i \\ 0, & \text{otherwise} \end{cases} \text{ for } i \in [1, r_{max}] \quad (24)$$

where, P represents the system's probability of surviving i number of hours; ts represents the total number of time steps (8760 for hourly analysis); h is the system's survival hours during an outage beginning in the i th hour (from the r series); hrs_i is the total number of survival hours for which the probability is being determined; r_{max} represents the maximum sustained hours of the system (for an outage beginning from a specific hour of the year derived from the index of r_{max} in the series). The preceding equation determines the system's probabilities of sustaining an outage length in the range from 1 to r_{max} . To account for the impact of the outage start hour and start month on the outage survival length, these probabilities are averaged over the hour of the day (for all 24 h) and the month of the year (for all 12 months).

3. Results and Discussions:

In order to determine the optimal size and operation of the integrated distributed energy resources (DER), for example, a PV-battery system combined with CHP units, the mMG model is both developed and simulated in this study. Two scenarios, financial and resilience, have been considered in this study and compared with business-as-usual

scenarios (BaU). It is found that the resilient system consists of 3933 kW of PV, 4441 kWh of storage, and a CHP unit having a capacity of 208 kW. The system comprises 2747 kW PV and 208 kW of CHP in the financial scenario. Only the grid supplied the electricity in the BaU scenario. Annual electricity supplied by the grid is 2,763,060 kWh in the resilience scenario compared to 8,981,110 kWh in the BaU scenario (Table 1). PV's average annual energy production is 6,138,498 kWh, while the CHP produces 1,344,622 kWh of electricity in the resilience scenario. The thermal energy produced by the CHP system is 5279 MMBtu (Table 1). To produce this energy, the amount of fuel consumed by the heating system is 14,293 MMBtu. In the BaU scenario, the grid emits 5919 tons of CO₂ annually, 79.81% higher than the resilient scenario. The resilient system has a net present value of \$1,007,204, which is 60% less than the financial scenario. The payback period and internal rate of return of the system are 11.86 years and 8.7%. The total LCC of the resilient system is \$6,954,339, which is 12 % less than the BaU scenario (Table 1).

Table 1. Comparison among three scenarios with a shutdown at 9 a.m. for 24 h during the peak month.

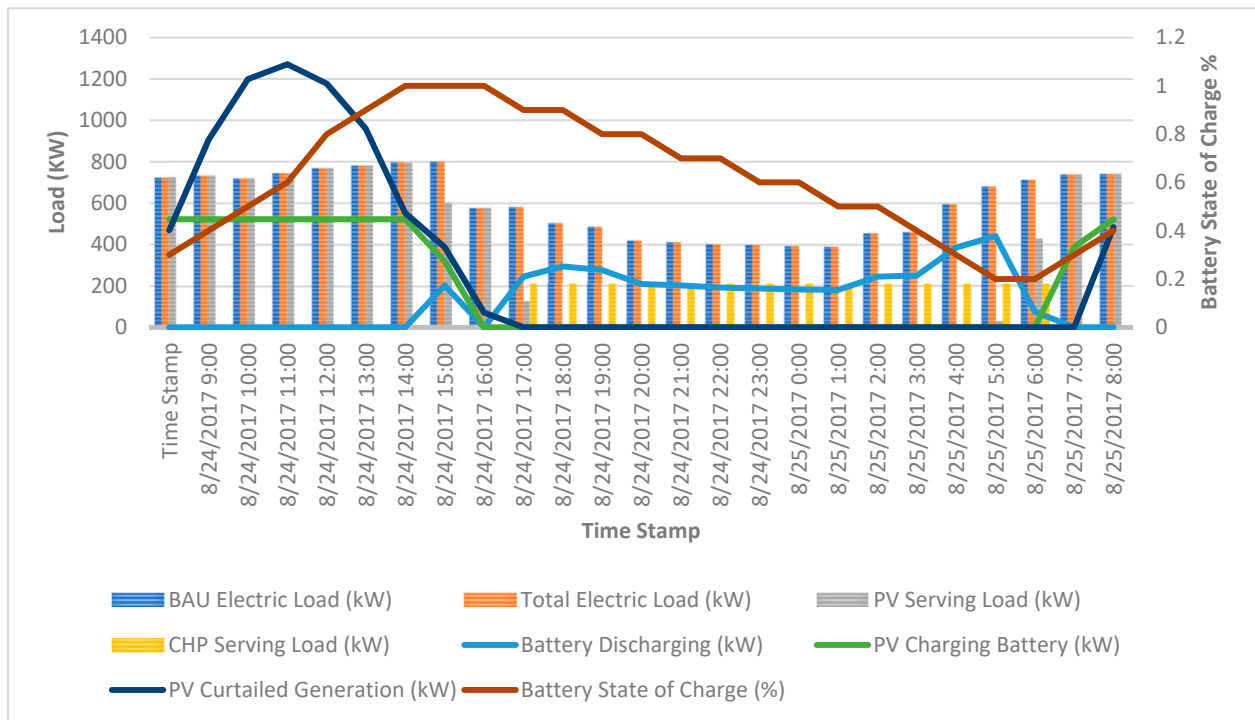
Parameters	Business as Usual (BaU)	Resilience	Financial
Average Annual PV Energy Production	-	6,138,498 kWh	4,288,000 kWh
Average Annual Energy Supplied from Grid	8,981,110 kWh	2,763,060 kWh	4,096,295 kWh
CHP Electric Production	-	1,344,622 kWh	1,379,199 kWh
CHP Thermal Production	-	5279 MMBtu	5386 MMBtu
Total CO ₂ Emissions in Year 1	5919 tons	2587 tons	3409 tons
Lifecycle Costs of Climate Emissions	\$549,080	\$987,294	\$1,000,613
Lifecycle Costs of Health Emissions	\$1,453,936	\$553,077	\$785,572
Utility Energy Cost	\$664,602	\$204,466	\$303,126
Total Life Cycle Costs	\$7,961,543	\$6,954,339	\$5,465,994
Payback Period	N/A	11.86 years	3.69 years
Internal Rate of Return	N/A	8.7%	24.6%

Observing the microgrid's performance during the outage period is required to ensure the designed microgrid can endure the outage and supply electricity to the load. Therefore, a 24-h outage starting at 9 AM in the peak month of August is scheduled to check the grid performance. During the fault condition, the grid does not serve the load. This situation exists till the grid comes into operation. The boiler and PV fulfil the electrical and thermal load during this time. After 5 PM, the boiler stopped serving the load, and CHP came into operation. CHP serves the load until 7 AM the following day.

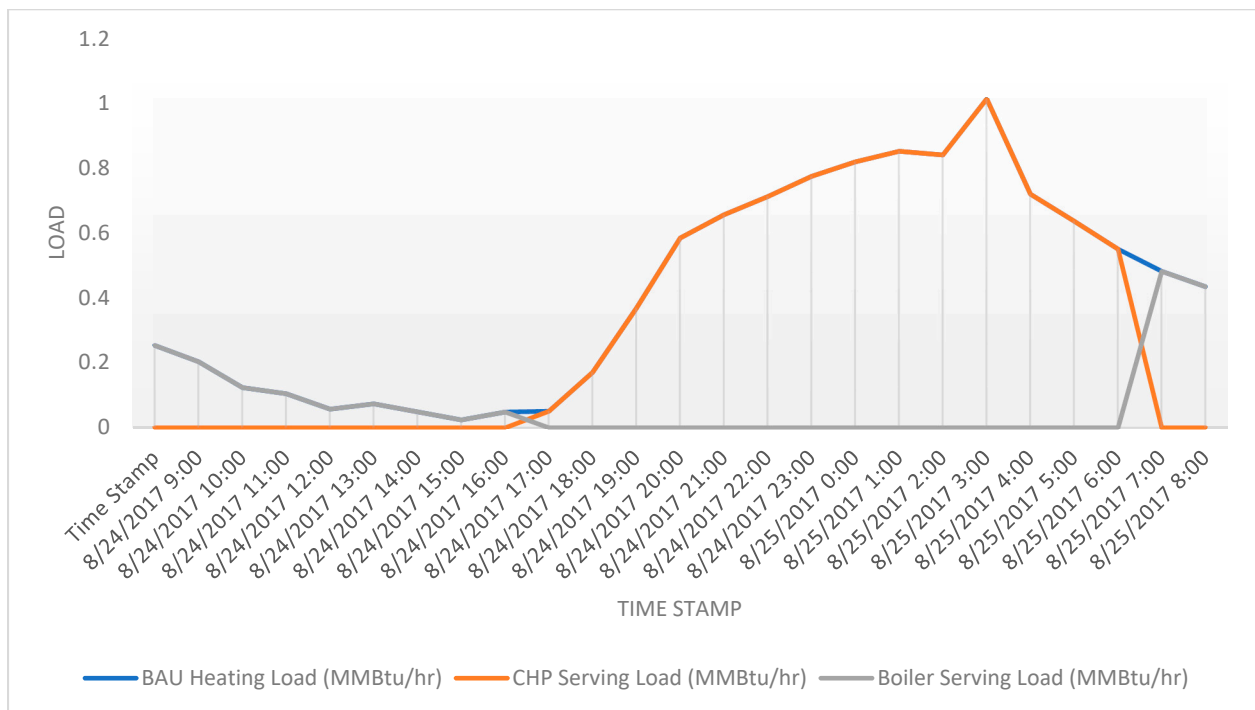
It should be noted that the battery's state of charge falls and rises exceptionally fast. It means batteries can deliver or charge roughly half their appraised limit in only one hour. There will be a time when there is low solar radiation during the day and no solar radiation at night. The PV module will be unable to generate less or no electricity during this period. The storage will fulfil the load until the PV produces electricity again. The performance of the micro-grid can be found in Figure 5.

A comparison of resilience benefits has been made among three scenarios and can be found in Table 2. From Table 2, it is clear that both in the financial and BaU scenario, the system cannot endure the outage. The financial scenario has a high NPV value, which is the life cycle cost savings during the project's lifespan. However, this system cannot endure the outage. The average outage that can be endured in the financial scenario is 2 h. After 2 h, the system will not supply electricity to the load. The finding of this study is consistent with this following study. This study identified the energy resilience of a PV/diesel/battery system and found that the system can withstand a 72-h outage. Moreover, \$99,491 can be saved after implementing the system [26]. Another study also

implemented the PV/diesel/battery system in Boston airport and found that the system can survive 718 h of outage [27].



(a)



(b)

Figure 5. The performance of the microgrid during outage condition. (a) Dispatch strategy optimized by REopt for the specified outage period. (b) Thermal dispatch strategy optimized by REopt.

Table 2. Comparison of resilience benefits among three analyzed scenarios.

Parameter	Business as Usual (BaU)	Resilience	Financial
System	None	3933 kW PV 522 kW Battery with 4441 kWh capacity 208 kW CHP	2747 kW PV 168 kW CHP
Survive specific outage	No	Yes	No
Average	0	7919 h	2
NPV	0	\$1,007,204	\$2,522,075

The outage survivability of the system is expressed in Figure 6. The outage possibility of the system is considered in the peak month (August). This is because, during the summer season, thermal and electricity consumption is higher. Therefore, more load will be added in the system.



Figure 6. Outage survival possibility of the system.

From Figure 6, it is evident that as the time increases, the outage probability of the system decreases. The business case scenario, which is the absence of the microgrid, cannot stand against the outage. From this figure, it is clear that both the financial and resilient system can successfully withstand 1 h of outage. However, when the outage duration

increases, the chance of the financial system withstanding the outage decreases. The total averted outage cost following the system's implementation is \$36,995,183, considering the avoided outage cost of \$100 per kWh (Figure 7). As a result, life-cycle savings of 37.02 million USD will be observed in the project's lifetime.

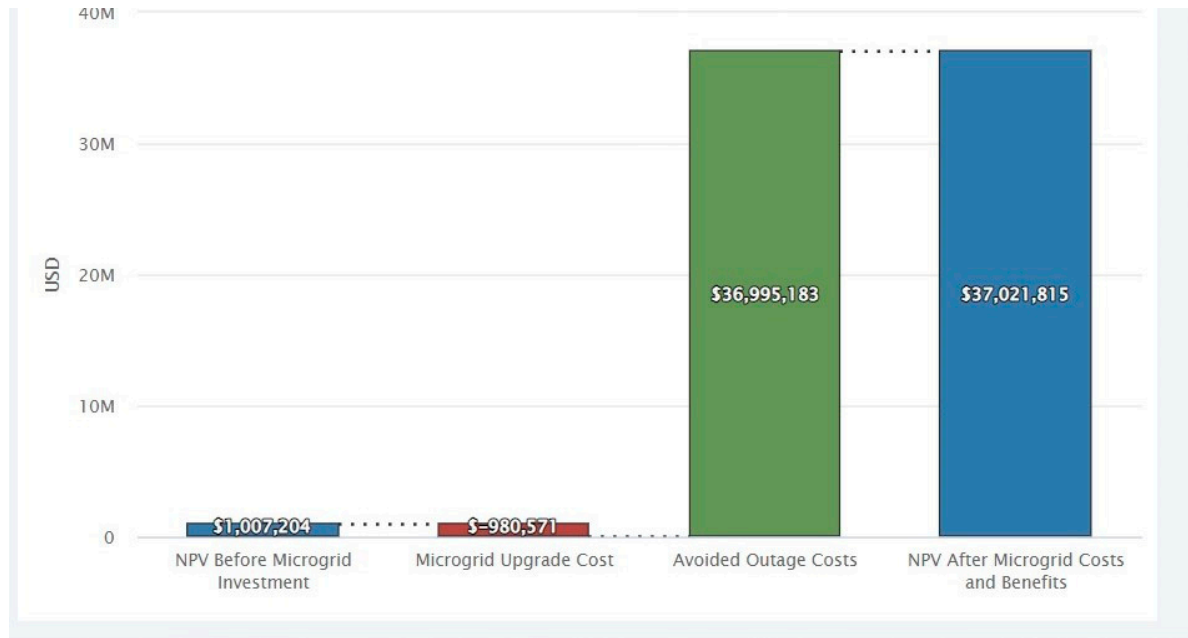


Figure 7. Cost saving after implementation of the micro-grid.

4. Conclusions

This study proposed a CHP system integrated with a PV/battery system for a hospital building in Texas, USA. The system runs successfully during the outage period, starting at 9 am and existing for 24 h. The proposed approach considers different pragmatic restrictions, making the objective function, i.e., minimizing the total cost, strong enough to endure the appointed outages. The optimum system consists of 3933 kW of PV, 4441 kWh of storage, and a CHP unit having a capacity of 208 kW. CHP contributes to meeting both heating and electricity demands while also reducing costs. PV and batteries work in a couple to tolerate the protracted blackout and thus ensure the hospital's uninterrupted and steady energy supply. Implementing this system can result in economic savings. The total outage cost that could be avoided after implementing the system is \$36,995,183. Over the project duration, the system has life-cycle savings of \$1,007,204. The outcome of this study will be helpful to states and cities as they work to improve public health and achieve climate goals while also increasing resilience to natural disasters. For example, resilience can be monetized and used to partially fund renewable energy hybrid systems by collaborating with organizations that have a stake in reducing risks, such as banks, insurance companies, and governmental agencies. Although this market still needs to be developed, it represents a multi-billion-dollar global opportunity.

A predefined outage is assigned to model the system, which can be considered a weakness of the present research. Future research should apply a stochastic technique to model the outage time and duration in the optimization module.

Author Contributions: Conceptualization, K.S.I.; Data curation, H.C.; Formal analysis, K.S.I.; Investigation, S.H.; Methodology, S.H. and T.C.; Project administration, H.C.; Resources, S.H.; Software, T.C.; Supervision, S.M.S.; Visualization, K.S.I.; Writing—original draft, T.C. and H.C.; Writing—review & editing, S.M.S. All authors have read and agreed to the published version of the manuscript.

Funding: This research received no funding.

Institutional Review Board Statement: Not applicable.

Informed Consent Statement: Not applicable.

Data Availability Statement: Not applicable.

Conflicts of Interest: The authors declare no conflict of interest.

Nomenclature

Abbreviations

DA	Days of autonomy.
DOD	Depth of charge of the battery.
STC	Standard test condition

Parameters

A_{PV}	Surface area of the PV module (m ²).
B^{kWh}	Battery capacity (kWh).
B^{kW}	Battery system size (kW).
B_{max}^{kWh}	Maximum storage capacity of the battery (kWh).
B^{SOCmin}	Minimum state of charge of battery (%).
B_h^+	In a time, step h, power delivered to the battery (kW).
B_h^-	In a time, step h, power dispatched from the battery (kW).
B_h^{SOC}	In a time, step h, energy stored in the battery (kW).
C_{Dn}	Demand cost.
C_{Eg}	Energy costs.
C_{OM}	Cost of operation & maintenance.
C_{PVBAT}	Capital cost of PV, battery.
c_t	Capital cost for technology t (\$/kW).
c_h^e	Electricity cost in time step h (\$/kW).
c_m^d	Demand cost for month m.
c_t^{OM}	O&M cost per unit size of the system for technology t (\$/kW).
$C_{P_{PV}}$	Rated capacity of PV array (kW).
c_r^d	Demand cost for ratchet r.
c_{kWh}^b	Capital cost of battery per kWh (\$/kWh).
c_{kW}^b	Capital cost of storage inverter per kW (\$/kW).
D_{PV}	Derating factor of solar PV array.
d_m	Monthly peak demand for month m (kW).
d_r	Peak demand in ratchet r (kW).
E_{load}	Average energy demand (kWh/day).
F_{dths}	Hourly capacity factor for demand d for energy technology t in time step h at locations s (unitless).
F_t^{dgr}	Degradation factor for technology t (unitless).
F_{tlh}^{pd}	Production factor for technology t, serving load l, in timestep h (unitless).
F_{ltsu}^f	Fixed fuel consumption.
F_{ltsu}^k	Varying fuel usage.
h_c^f	Consumption rate of the fuel, i.e., natural gas.
I_r	Solar irradiation on the PV panel's surface (kW/m ²).
I_{rsrc}	Solar irradiation under STC.
L_{lh}	Production size restriction for load l in time step h(kW).
L_{sv}^{NEM}	Capacity of net metering level v at location s.
P_{out}	Electric power generation from the CHP unit.
P_g	Grid power.
$P_l(t)$	Load power demand.
P_{PV}, P_{chp} and P_{batt}	Power supplied by the corresponding energy sources.
P_{tlh}	Rated production of technology t, serving load l, in timestep h (kW).
Q_{out}	Heat power generation from the CHP unit.
R	Both the fuel burn rate and available usable heat for electric (e) and heat generation (h).

$T_{C,STC}$	Temperature under STC.
T_C	PV cell temperature in the current time step ($^{\circ}\text{C}$).
X_t	System size for energy technology.
X_{tlh}^o	1 if the technology is active, else 0.
Y_{sv}	1 if location s is operated at the Net metering level v ; otherwise, 0.
α_P	Temperature coefficient of power (%/degree C).
$\eta_{con}n_{batt}$	Efficiency of converter and battery.
η_{STC}	Efficiency of the PV module under STC (%).
η_B	Efficacy of the roundtrip inverter.
η_e	Electric recovery efficiency of the CHP plant.
η_h	Heat recovery efficiency of the CHP plant.
Sets	
$t \in \mathcal{T}$	Set of energy technologies (solar PV = PV and G = grid).
$r \in \mathfrak{R}$	Set of all ratchets.
$m \in \mathcal{M}$	Set of all months.
$h \in \mathcal{H}$	Set of time steps
$l \in \mathcal{L}$	Set of loads, l^S for site load, l^B for Battery load, l^{Ex} for export.
$v \in V$	Set of net metering levels.
$u \in U$	Set of fuel bin.
$s \in S$	Set of all locations.

References

1. Increase in Natural Disasters on a Global Scale by Ten Times. Available online: <https://www.visionofhumanity.org/global-number-of-natural-disasters-increases-ten-times/> (accessed on 22 March 2022).
2. Natural Disasters Skyrocket in Texas. Available online: <https://spectrumlocalnews.com/tx/south-texas-el-paso/news/2022/04/20/natural-disasters-skyrocket-in-texas> (accessed on 1 October 2022).
3. Littlechild, S.; Kiesling, L. Hayek and the Texas blackout. *Electr. J.* **2021**, *34*, 106969. [CrossRef]
4. Schaefer, J.L.; Siluk, J.C.M.; de Carvalho, P.S. An MCDM-based approach to evaluate the performance objectives for strategic management and development of Energy Cloud. *J. Clean. Prod.* **2021**, *320*, 128853. [CrossRef]
5. Schaefer, J.; Siluk, J.; Carvalho, P.; Pinheiro, J.R.; Schneider, P. Management Challenges and Opportunities for Energy Cloud Development and Diffusion. *Energies* **2020**, *13*, 4048. [CrossRef]
6. Kemabonta, T. Grid Resilience analysis and planning of electric power systems: The case of the 2021 Texas electricity crises caused by winter storm Uri (#TexasFreeze). *Electr. J.* **2021**, *34*, 107044. [CrossRef]
7. Allahviridzadeh, Y.; Moghaddam, M.P.; Shayanfar, H. A survey on cloud computing in energy management of the smart grids. *Int. Trans. Electr. Energy Syst.* **2019**, *29*, e12094. [CrossRef]
8. Masrur, H.; Gamil, M.M.; Islam, R.; Muttaqi, K.M.; Lipu, M.S.H.; Senjyu, T. An Optimized and Outage-Resilient Energy Management Framework for Multicarrier Energy Microgrids Integrating Demand Response. *IEEE Trans. Ind. Appl.* **2022**, *58*, 4171–4180. [CrossRef]
9. Ogunmodede, O.; Anderson, K.; Cutler, D.; Newman, A. Optimizing design and dispatch of a renewable energy system. *Appl. Energy* **2021**, *287*, 116527. [CrossRef]
10. McLaren, J.; Laws, N.; Anderson, K.; DiOrio, N.; Miller, H. Solar-plus-storage economics: What works where, and why? *Electr. J.* **2019**, *32*, 28–46. [CrossRef]
11. Marqusee, J.; Becker, W.; Ericson, S. Resilience and economics of microgrids with PV, battery storage, and networked diesel generators. *Adv. Appl. Energy* **2021**, *3*, 100049. [CrossRef]
12. Hussain, A.; Bui, V.-H.; Kim, H.-M. Resilience-Oriented Optimal Operation of Networked Hybrid Microgrids. *IEEE Trans. Smart Grid* **2017**, *10*, 204–215. [CrossRef]
13. Khodaei, A. Resiliency-Oriented Microgrid Optimal Scheduling. *IEEE Trans. Smart Grid* **2014**, *5*, 1584–1591. [CrossRef]
14. Lagrange, A.; de Simón-Martín, M.; González-Martínez, A.; Bracco, S.; Rosales-Asensio, E. Sustainable microgrids with energy storage as a means to increase power resilience in critical facilities: An application to a hospital. *Int. J. Electr. Power Energy Syst.* **2020**, *119*, 105865. [CrossRef]
15. Laws, N.D.; Anderson, K.; DiOrio, N.A.; Li, X.; McLaren, J. Impacts of valuing resilience on cost-optimal PV and storage systems for commercial buildings. *Renew. Energy* **2018**, *127*, 896–909. [CrossRef]
16. Rosales-Asensio, E.; de Simón-Martín, M.; Borge-Diez, D.; Blanes-Peiró, J.J.; Colmenar-Santos, A. Microgrids with energy storage systems as a means to increase power resilience: An application to office buildings. *Energy* **2019**, *172*, 1005–1015. [CrossRef]
17. Anderson, K.; Grymes, J.; Newman, A.; Warren, A. North Carolina Water Utility Builds Resilience with Distributed Energy Sources. *Inf. J. Appl. Anal.* **2022**. [CrossRef]

18. Anderson, K.; Farthing, A.; Elgqvist, E.; Warren, A. Looking beyond bill savings to equity in renewable energy microgrid deployment. *Renew. Energy Focus* **2022**, *41*, 15–32. [[CrossRef](#)]
19. Hervás-Zaragoza, J.; Colmenar-Santos, A.; Rosales-Asensio, E.; Colmenar-Fernández, L. Microgrids as a mechanism for improving energy resilience during grid outages: A post COVID-19 case study for hospitals. *Renew. Energy* **2022**, *199*, 308–319. [[CrossRef](#)]
20. Sepúlveda-Mora, S.B.; Hegedus, S. Resilience analysis of renewable microgrids for commercial buildings with different usage patterns and weather conditions. *Renew. Energy* **2022**, *192*, 731–744. [[CrossRef](#)]
21. Masrur, H.; Islam, R.; Muttaqi, K.M.; Gamil, M.M.; Huang, Y.; Senjyu, T. Resilience-aware Optimal Design and Energy Management Scheme of Multi-energy Microgrids. In Proceedings of the 2021 IEEE Industry Applications Society Annual Meeting (IAS), Vancouver, BC, Canada, 10–14 October 2021; Institute of Electrical and Electronics Engineers Inc.: Piscataway, NJ, USA, 2022; pp. 1–5. [[CrossRef](#)]
22. REopt Mathematical Model Documentation. Available online: https://github.com/NREL/REopt_API/wiki/REopt-Mathematical-Model-Documentation (accessed on 17 March 2022).
23. Das, B.K.; Al-Abdeli, Y.M.; Kothapalli, G. Integrating renewables into stand-alone hybrid systems meeting electric, heating, and cooling loads: A case study. *Renew. Energy* **2021**, *180*, 1222–1236. [[CrossRef](#)]
24. Hossain, A.; Pota, H.R.; Squartini, S.; Abdou, A.F. Modified PSO algorithm for real-time energy management in grid-connected microgrids. *Renew. Energy* **2019**, *136*, 746–757. [[CrossRef](#)]
25. Mishra, S.; Anderson, K. Probabilistic Resilience of DER Systems—A Simulation Assisted Optimization Approach. In Proceedings of the 2021 IEEE Power & Energy Society Innovative Smart Grid Technologies Conference (ISGT), Washington, DC, USA, 16–18 February 2021; Institute of Electrical and Electronics Engineers Inc.: Piscataway, NJ, USA, 2021; pp. 1–5. [[CrossRef](#)]
26. Arefin, A.A.; Masrur, H.; Othman, M.L.; Hizam, H.; Wahab, N.I.A.; Jalaluddin, N.A.; Islam, S.Z. Power Resilience Enhancement of a PV- Battery-Diesel Microgrid. In Proceedings of the 2020 International Conference on Smart Grids and Energy Systems (SGES), Perth, Australia, 23–26 November 2020; Institute of Electrical and Electronics Engineers Inc.: Piscataway, NJ, USA, 2021; pp. 860–863. [[CrossRef](#)]
27. Masrur, H.; Sharifi, A.; Islam, R.; Hossain, A.; Senjyu, T. Optimal and economic operation of microgrids to leverage resilience benefits during grid outages. *Int. J. Electr. Power Energy Syst.* **2021**, *132*, 107137. [[CrossRef](#)]